Materials Science & Engineering C 117 (2020) 111296

Contents lists available at ScienceDirect

Materials Science & Engineering C

journal homepage: www.elsevier.com/locate/msec

Catalase immobilized antimonene quantum dots used as an electrochemical biosensor for quantitative determination of H_2O_2 from CA-125 diagnosed ovarian cancer samples

Batool Fatima[a], Dilshad Hussain[b,c], Shazia Bashir[a], Hafiza Tanzilla Hussain[b], Rashida Aslam[a], Rahat Nawaz[b], Hafiza Nadia Rashid[b], Nabila Bashir[b], Saadat Majeed[b], Muhammad Naeem Ashiq[b], Muhammad Najam-ul-Haq[b,*]

[a] Department of Biochemistry, Bahauddin Zakariya University, Multan 60800, Pakistan
[b] Division of Analytical Chemistry, Institute of Chemical Sciences, BahauddinZakariya University, Multan 60800, Pakistan
[c] HEJ Research Institute of Chemistry, International Centre for Chemical and Biological Sciences, University of Karachi, Karachi 75270, Pakistan

ARTICLE INFO

Keywords:
Antimonene quantum dots
Catalase
Electrochemical sensing
Hydrogen peroxide
CA125
Ovarian cancer

ABSTRACT

A selective and cost-effective biosensor based on catalase immobilized antimonene quantum dots modified glassy carbon electrode (Cat@AMQDs-GCE) is designed for the first time to determine hydrogen peroxide (H_2O_2). Antimonene quantum dots (AMQDs) are synthesized by a single step method, characterized by various analytical techniques and applied to the electrochemical sensing of hydrogen peroxide. Catalase enzyme specific for H_2O_2 reduction is immobilized onto AMQDs to facilitate its detection by cyclic voltammetry and amperometry. Concentration, scan rate, pH, stability and selectivity are optimized. Linearity of Cat@AMQDs-GCE is determined as 0.989 with limit of detection as 4.4 μM. Amperometric measurements show recovery of 95 to 103.4% for H_2O_2 from human serum samples. Cat@AMQDs-GCE is electrochemically stable up to 30 cycles, reducing the cost of analysis. Cat@AMQDs-GCE shows good selectivity in presence of ascorbic acid, dopamine, leucine and glucose. Prepared electrode is also applied for the quantitative determination of H_2O_2 from ovarian cancer serum. CA 125 concentration is previously determined by Elecsys CA 125 II Assay. Results demonstrate that concentration of H_2O_2 increases with increasing levels of CA125 in serum.

1. Introduction

According to recent reports, cancer has become the leading cause of death in women throughout the World. There were estimated 3.5 million annual deaths among females worldwide in 2012 and this number is expected 5.5 million by 2030 [1]. Breast, ovarian and cervical cancers are increasing due to environmental, hormonal and virus factors. These causative factors are associated with oxidative stress (OS) which increases by the formation of reactive oxygen species (ROS) [2]. Analysis of epidemiological and experimental data shows the production of ROS creating imbalance between oxidants and antioxidants defense mechanism. Chronic oxidative stress causes mutation in genes by changing the expression of cancer related genes which lead to cancer [3]. ROS comprise of highly reactive hydroxyl radical, hydrogen peroxide, singlet oxygen and superoxide anion radical [4–6].

Hydrogen peroxide is an important component of living cells having role in the host defense system and biosynthetic oxidation reactions. H_2O_2 at lower concentrations functions as signaling component in living organisms [7]. It is fast moving and can pass through cell and nuclear membranes [8]. Balance of H_2O_2 inside the living body is maintained by an enzyme called catalase [9]. H_2O_2 itself is a reactive metabolite rather than a free radical. Its lower concentration is even toxic to living cells [10]. It is further linked to DNA damage, mutation and instability of genetic material. Studies reveal that H_2O_2 induces apoptosis, cell proliferation, enhanced angiogenesis and metastasis [11]. Chemical antioxidants interact with antioxidant enzymes and protect living cells against oxidative stress. In oxidative phosphorylation, hydrogen peroxide is produced from superoxide which is further reduced to water and oxygen [12]. This detoxification results from the combined action of multiple enzymes like superoxide dismutase which catalyzes the first step and catalases and peroxidases which remove hydrogen peroxide [13].

H_2O_2 is the by-product of oxidative enzymes [14]. A specific and sensitive technique for its detection is necessary. Detection of tumor

* Corresponding author at: Institute of Chemical Sciences, BahauddinZakariya University, Multan 60800, Pakistan.
E-mail address: najamulhaq@bzu.edu.pk (M. Najam-ul-Haq).

https://doi.org/10.1016/j.msec.2020.111296
Received 10 February 2020; Received in revised form 23 June 2020; Accepted 21 July 2020
Available online 24 July 2020
0928-4931/

biomarkers like H_2O_2 has role in medical diagnoses of tumor-linked diseases [15]. Numerous methods have been reported for the detection of hydrogen peroxide including fluorescence [16], flow cytometry [17], chemiluminescence [18], and colorimetric assay [19]. Commercial kits have been used in clinical immunoassays however with limitations. Electrochemical techniques are developed for the measurement of hydrogen peroxide with real-time analysis and direct measurement [20–22]. Biosensors determine H_2O_2 selectively and sensitively by transferring electron from proteins like cytochrome *c* (cyt c) [23], myoglobin (Mb) [24], horseradish peroxidase (HRP) [25], and hemoglobin (Hb) [26]. Moreover, electrodes modified with inorganic materials detect H_2O_2 due to their stability and better electron transfer [27]. Inorganic materials used for hydrogen peroxide sensors include silver nanoparticles [28], carbon based nanocomposites [29], palladium nanoparticles on graphene oxide nanosheets [30], CuO nanoflowers [31], TiO_2 nanoparticles [32], Pd/PEDOT nanocomposite [33], CuO@Cu_2O nanowires embedded into poly(vinyl alcohol) [34], cerium oxide nanoparticles [35], Se/Pt nanocomposite [36] and polyethyleneimine-capped silver nanoclusters [37].

In this study, an electrochemical sensor based on Cat@AMQDs-GCE is developed and used as an enzymatic biosensor for the quantitative detection of H_2O_2. Antimonene quantum dots, used for the first time in sensing applications, are selected due to its inherent anticancer properties. Some other types of quantum dots include black phosphorous [38,39], Ag_2S [40] and copper nanoclusters [41] which have been recently used in sensing applications. AMQSs have been previously reported for other applications including Li storage [42], NIR photothermal therapy [43], SPR sensors [44] and as bi-dimensional materials [45]. Higher surface area of AMQDs and immobilized catalase can be an effective combination for sensing of hydrogen peroxide. The immobilized catalase has electrocatalytic activity towards H_2O_2 reduction. Developed sensor is also applied to determine H_2O_2 from CA125 ovarian cancer serum samples. CA125 level in ovarian cancer patients is determined by Cobass E411 Assay. The study proves higher tumor stage associated with the higher level of CA125 which is directly related to higher production of H_2O_2 in ovarian cancer samples.

2. Experimental

2.1. Chemicals and reagents

Powdered antimony-100 mesh, hydrogen peroxide, ascorbic acid, leucine, dopamine, glucose and ethanol were purchased from Sigma Aldrich. 1,2-Distearoyl-sn-glycero-3-phosphoethanolamine-N(methoxy polyethylene glycol) (DSPE-PEG) was obtained from Avantipolar Lipid. All the chemicals were of analytical grade and used without any further pretreatment.

2.2. Synthesis of antimonene quantum dots

Antimonene quantum dots (AMQDs) were synthesized by the combination of probe and bath sonication techniques through fling or interjection in ethanol [43]. 500 mg antimony powder was taken in a beaker and 20 mL ethanol was added. Mixture was sonicated for 10 h in ice bath with power set as 500 W, for 6 h at 300 W and for 5 h at 500 W. Mixture was then centrifuged for 20 min at 3000 rpm. The supernatant contained AMQDs which were characterized and used for electrochemical analysis.

2.3. Electrochemical sensing of hydrogen peroxide by Cat@AMQDs-GCE

Redox activity of Cat@AMQDs-GCE was recorded by cyclic voltammetry (AUT50296, Autolab Potentiostat) using three electrodes system; reference electrode, platinum wire and working electrode in a glass cell of volume 100 mL [46]. Ag/AgCl was used as reference electrode. Modified glassy carbon electrode with Cat@AMQDs was used as working electrode for H_2O_2 sensing. Working electrode was cleaned by sonication for 15 min. Procedure was repeated thrice with soap and distilled water and dried in oven. AMQDs (5 mg) and catalase (5 mg) were mixed in the ratio of 1:1 (w/w) and grinded to obtain homogenous pastein 2 mL ethanol and filled in electrode. Solution of different concentrations of H_2O_2 was prepared in PBS (pH 7). All the measurements were made at room temperature.

2.4. Elecsys CA 125 II assay

The Elecsys CA 125 II tumor marker assay is a specific immunoassay based on two monoclonal antibodies (OC 125 and M 11), available at Fujirebio Diagnostics. Blood samples of 14 ovarian cancer patients were collected in commercial sample collection tubes. Sandwich Elisa principle was applied for the detection of CA125 antigen. The assay was applied for 18 min. 20 µL plasma sample was taken for 1st incubation. 1 $mg.mL^{-1}$ biotinylated monoclonal CA 125 specific antibody (M11; mouse) preserved in 100 $mmol.L^{-1}$ phosphate buffer formed sandwich complex with monoclonal CA 125 specific antibody (OC 125; mouse) labeled as1$mg.L^{-1}$ preserved in 100 $mmol.L^{-1}$ phosphate buffer ruthenium complex at pH 7.4. In 2nd incubation, solid phase was attached to 0.72 $mg.mL^{-1}$ streptavidin coated microparticles complex using streptavidin and biotin interactions. This mixture of microparticles bound to solid phase was aspirated into the measuring cell, followed by magnetic capturing of microparticles onto the surface of electrode. Removal of unbound substrate was done by ProCell/ProCell M. Chemiluminescent emission was induced by applying voltage to the electrode. Photomultiplier detector measured the emission intensity and calibration curve was automatically drawn with two point calibration. Results were evaluated and CA 125 level was determined from the curve.

3. Results and discussion

3.1. Synthesis and characterization of antimonene quantum dots (AMQDs)

Cancer must be addressed appropriately and timely to decrease the burden of disease and to confront gender inequalities [47]. Detection of hydrogen peroxide as tumor marker is important in clinical research. Catalase being the specific enzyme only catalyzes H_2O_2 into water and oxygen [48]. Mechanism of action of catalase is unique where one molecule of H_2O_2 oxidizes the co-factor of catalase, followed by the transfer of bound oxygen from second molecule, resulting in regeneration of co-factor. Reaction process is given in Eq. (1).

$$2H_2O_2 \xrightarrow{Catalase} 2H_2O + O_2 \quad (1)$$

Catalysis of hydrogen peroxide is based on electron transfer mechanism. AMQDs act as accelerator and facilitator for electrons transfer. In Cat@AMQDs-GCE, catalase offers functional specificity and AMQDs work as electrochemical transducers facilitating the electrons transfer and signals.

Synthesized quantum dots are characterized by TEM, AFM, SEM, EDS, FTIR and XRD. TEM images of AMQDs demonstrate that particles are irregular shaped with size less than 20 nm (Fig. 1A). Similar pattern and particle sizes (8–12 nm) are observed in AFM (Fig. 1B). SEM image shows irregular morphology with slight agglomeration which can happen upon drying the particles on conductive carbon tape for SEM analysis (Fig. 1C). EDS analysis verifies the composition of AMQDs showing 98.33 atomic percent of antimony (Fig. 1D). X-ray diffraction is performed for the qualitative analysis in diffraction range of 5–120° [2θ] which shows the crystallinity of material with characteristic peaks at 24, 29.5, 40, 42, 48.5 and 52 (Fig. 1E). FTIR analysis reveals peaks at 412 cm^{-1} and 1097 cm^{-1} for the antimony (Fig. 1F) [43].

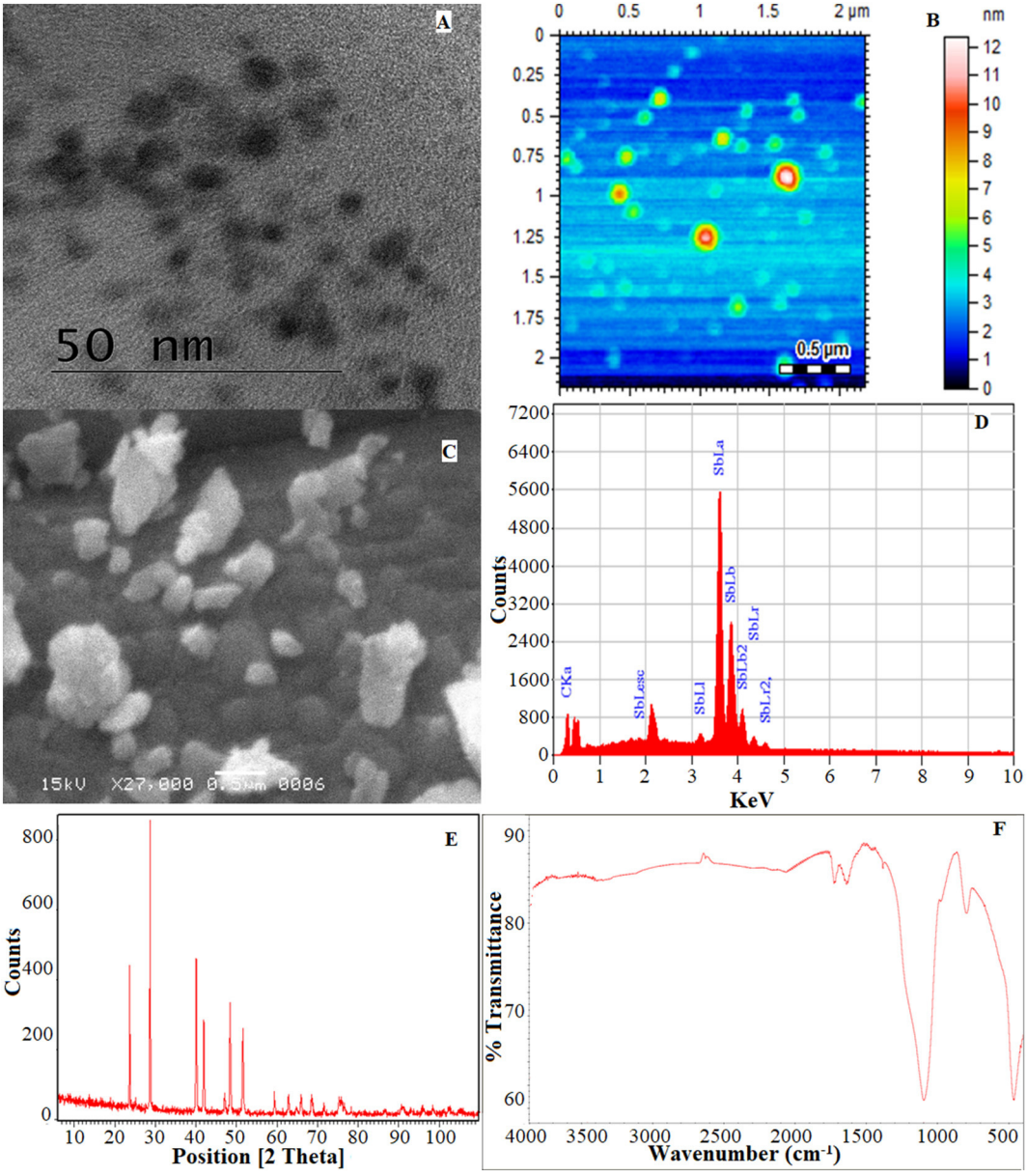

Fig. 1. Characterization of antimonene quantum dots (A) TEM (B) AFM (C) SEM (D) EDS (E) XRD and (F) FTIR.

3.2. Electrochemical performance of Cat@AMQDs-GCE

Electrochemical characterization of Cat@AMQDs-GCE is done using cyclic voltammetry (CV). Fig. 2A shows the CV curves for standardization of modified electrode in 0.1 M potassium ferrocyanide containing 0.1 M KCl solution. Red line shows the conductivity of bare GCE in potassium ferrocyanide solution. No prominent oxidation and reduction peaks observed in bare GCE. Black curve shows the voltammetric response of Cat@AMQDs-GCE in potassium ferrocyanide solution. A broad oxidation peak is observed at potential +0.7 V. Two reduction peaks at potential −0.9 V and −0.3 V show redox activity of Cat@AMQDs-GCE. The enzyme modified electrode is then applied for the sensing of H_2O_2. Fig. 2B shows the redox activity of modified electrode in 0.1 M PBS (pH 7) and also in 1 mM solution of H_2O_2 in PBS. No oxidation reduction is observed in PBS without hydrogen peroxide whereas oxidation and reduction peaks are observed at potential +1.0 V and −0.9 V respectively in 0.1 M PBS containing 1 mM H_2O_2.

Cat@AMQDs-GCE is applied in various pH conditions (4, 5, 6, 7 and 8) to check the pH effect on sensing of hydrogen peroxide and results are shown in Fig. 3A. With the increase in pH from 4 to 7, current produced by 1 mM solution of H_2O_2 in 0.1 M PBS also increases. Above pH 7, current decreases and at pH 9, electrode material is unstable (Fig. 3B). pH 7 is thus chosen to study the other CV parameters for sensing of H_2O_2. This further demonstrates that Cat@AMQDs-GCE works best under physiological conditions and can be useful for the determination of hydrogen peroxide in real biological samples.

Scan rate is optimized for the best redox conditions of 1 mM H_2O_2 at scan rates 0.01 mV/s to 0.06 mV/s in 0.1 M PBS (pH 7) (Fig. 4A). Current increases constantly by increasing the scan rate. Minimum current is noted for 0.01 mV/s and maximum at 0.06 mV/s showing linearity between current and scan rate (Fig. 4B). There is also direct relation between current and potential for produced current because of reduction and oxidation at various scan rates. Maximum reduction current and minimum oxidation current are noted at 0.01 mV/s while minimum reduction current and maximum oxidative current at 0.06 mV/s. R^2 values for reduction and oxidation are 0.9305 and 0.9829 respectively.

Concentration effect of hydrogen peroxide at Cat@AMQDs-GCE is also optimized. Fig. 5A shows CV results in concentrations of 1 to 6 mM.

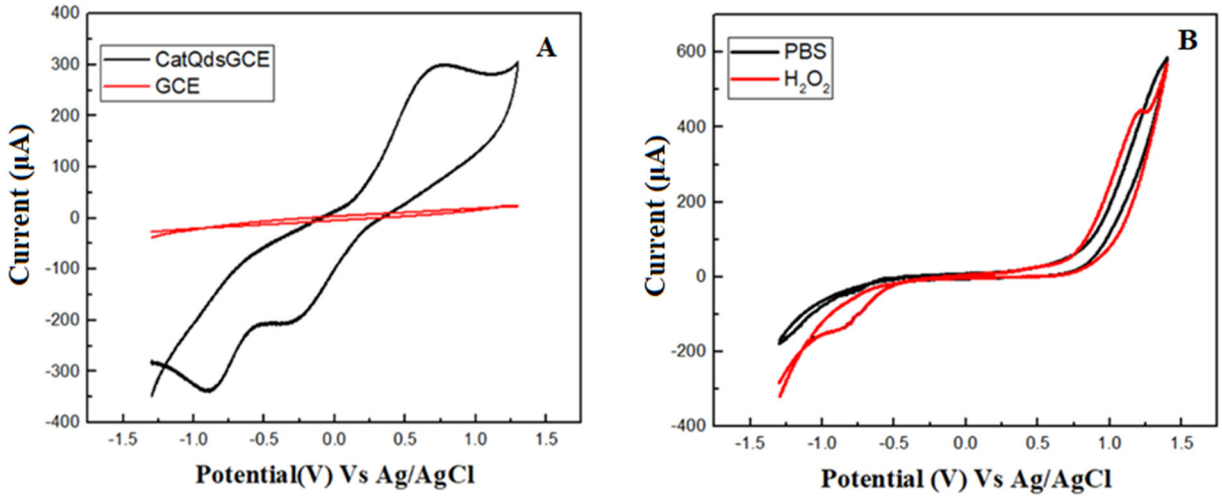

Fig. 2. (A) Cyclic voltammetric behavior of potassium ferrocyanide at bare glassy carbon electrode and Cat@AMQDs-GCE (B) Cyclic voltammetry of Cat@AMQDs-GCE of 1 mM solution of H_2O_2 in 0.1 M PBS and blank 0.1 M PBS.

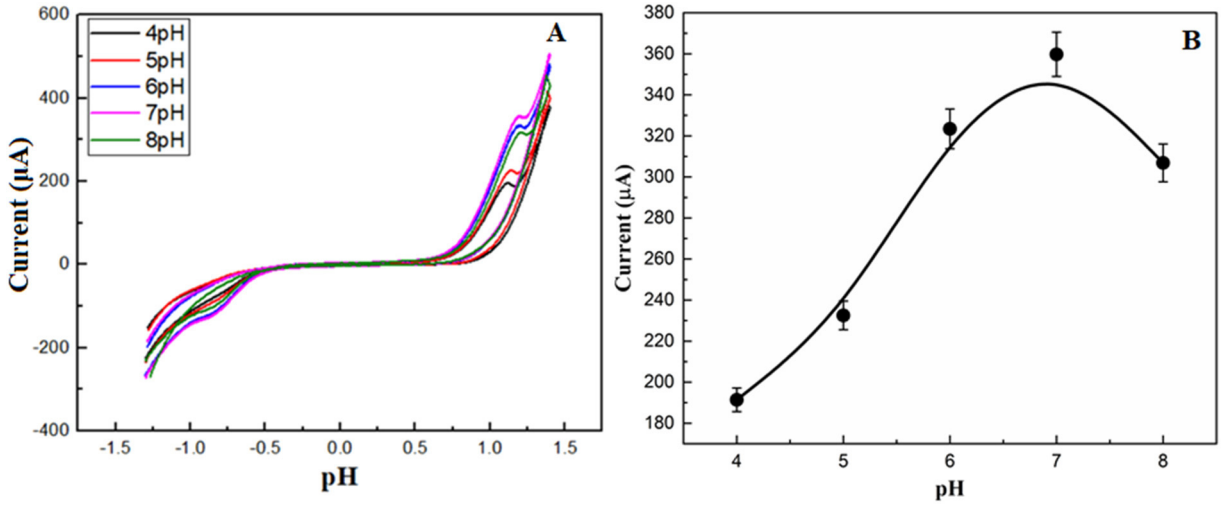

Fig. 3. (A) Cyclic voltammogram showing redox behavior of 1 mM solution of H_2O_2 at Cat@AMQDs-GCE at pH 4, 5, 6, 7 and 8 in 0.1 M PBS, (B) corresponding line graph. Conditions: 1 mM solution of H_2O_2 in 0.1 M PBS, potential window −1.5 V to +1.5 V, Scan rate 0.01 mV/s.

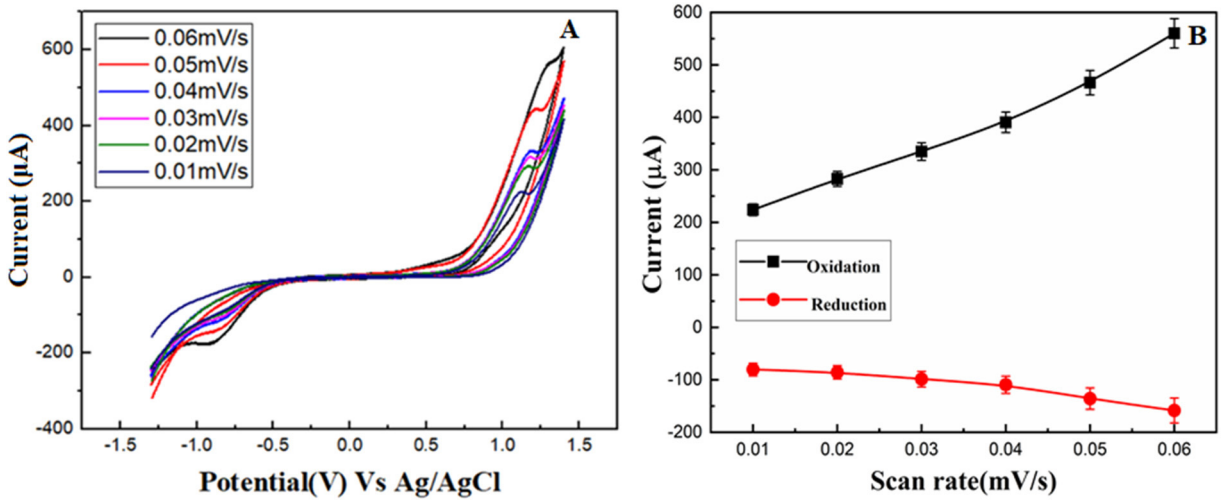

Fig. 4. (A) Cyclic voltammogram showing the electrochemical behavior of Cat@AMQDs-GCE towards 1 mM hydrogen peroxide at different scan rates in 0.1 M PBS of pH 7. Conditions: potential window −1.5 V to +1.5 V, Scan rate 0.01, 0.02, 0.03, 0.04, 0.05, and 0.06 mV/s. (B) Corresponding calibration graph.

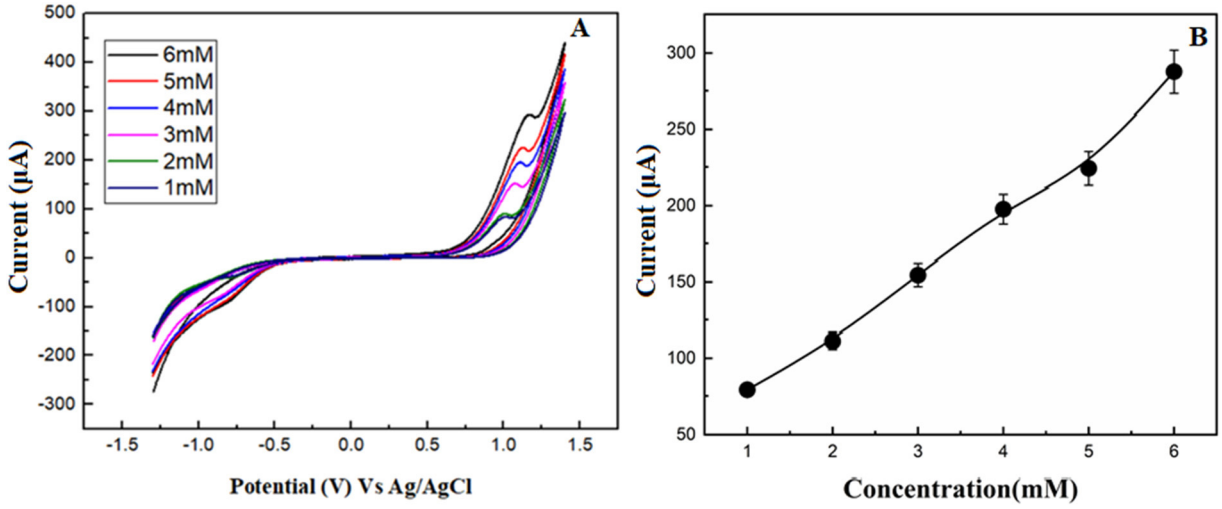

Fig. 5. (A) Cyclic voltammogram showing the redox behavior of H_2O_2 at Cat@AMQDs-GCE of different concentrations of hydrogen peroxide in 0.1 M PBS of pH 7. Conditions: potential window −1.5 V to +1.5 V, Scan rate 0.01 mV/s. (B) Corresponding calibration graph.

Oxidation peak current increases by increasing analyte concentration. Maximum current is observed at 6 mM while least oxidation peak current is at 1 mM concentration of H_2O_2 in 0.1 M PBS of pH 7. Fig. 5B indicates direct relation between concentration of hydrogen peroxide and current. The modified electrode has linear dependency of $R^2 = 0.98999$.

Effect of interferences is tested by adding interfering species in 1 mM H_2O_2 solution. Ascorbic acid and glucose are added first in same concentration as of H_2O_2 and then their concentrations are increased two times as compared to H_2O_2. Oxidation peak of H_2O_2 becomes less prominent by adding interfering species, however there is one other peak detected at potential −0.4 V (Fig. S1). This peak may be due to presence of ascorbic acid. Cat@AMQDs-GCE has good selectivity for H_2O_2 sensing.

Stability of modified electrode is evaluated by setting 30 cycles of cyclic voltammetry for 1 mM H_2O_2 in 0.1 M PBS of pH 7 (Fig. S2). After passing thirty cycles, both oxidation and reduction peaks are obtained at same potential as for the first cycle. Electrode material can thus be reused efficiently with high reproducibility.

3.3. Amperometric analysis of H_2O_2 by Cat@AMQDs-GCE

Amperometry checks the effect of change in concentration of target analyte on Cat@AMQDs-GCE. Current response increases with the increasing concentration (from 50 to 300 μM) of hydrogen peroxide under potential −0.1 V in 0.1 M PBS (pH 7) and attains a steady state (Fig. 6A). The calibration curve is linear for current to the concentration of H_2O_2 with R^2 0.9791 and limit of detection (LOD) as 4.4 μM (Fig. 6B). Cat@AMQDs-GCE has better sensing ability as compared to some previous studies (Table S1).

Interference effect of other species is optimized by applying the amperometric method to know the selectivity of Cat@AMQDs-GCE. Ascorbic acid (AA), leucine, dopamine (DA), and glucose are used as interfering species. Fig. S3 shows no obvious change of current with these species.

3.4. Recovery analysis of H_2O_2 by Cat@AMQDs-GCE

The applicability of Cat@AMQDs-GCE to real samples is evaluated by determining the recovery of spiked hydrogen peroxide in human serum. Serum is diluted twenty times with PBS solution of pH 7. Recovery of hydrogen peroxide is measured in the serum by spiking

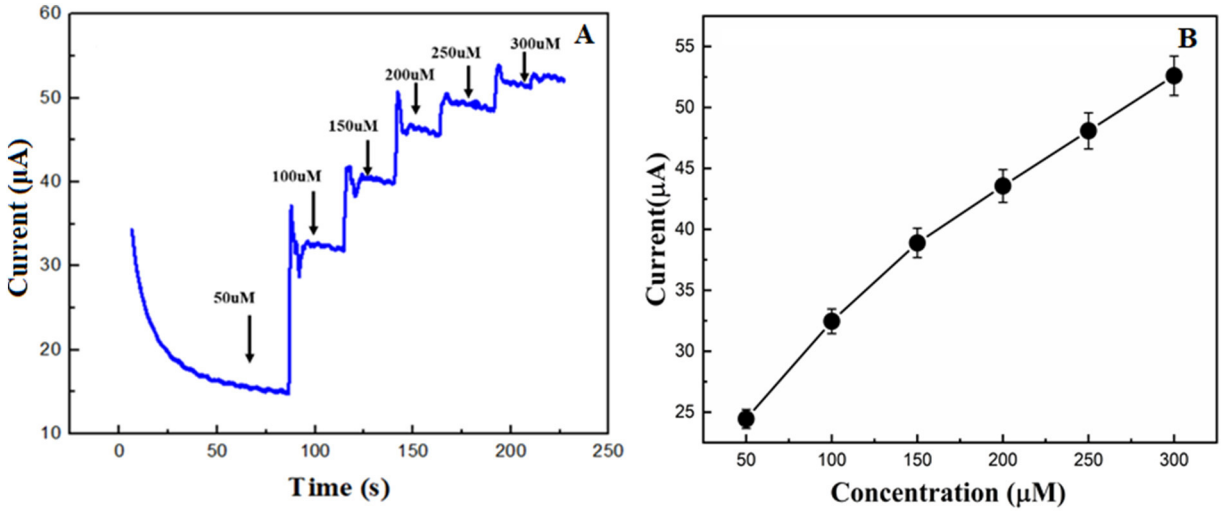

Fig. 6. (A) Amperometric response of Cat@AMQDs-GCE with different concentrations of H_2O_2 in 0.1 M PBS of pH 7 (applied potential: −0.5 V to +0.5 V). (B) Corresponding linear graph.

Table 1
Results of standard addition and recoveries from human blood serum.

Samples	Added conc. (mM)	Found conc. (mM)	Recovery (%)
1	1	0.95	95
2	5	4.87	97
3	10	9.89	98
4	15	15.29	101
5	20	20.68	103.4

Table 2
Levels of CA125 (obtained from Elecsys CA 125 II Assay) and H_2O_2 (calculated after sensing by Cat@AMQDs-GCE) from serum samples of ovarian cancer patients.

Sample no.	CA125 (units/mL)	Current (μA)	Conc. of H_2O_2 (μM)	Scan rate (mV/s)	Potential window (V)
1	5.1	3.56	5.31	0.01	−1.5 to +1.5
2	11.6	5.73	8.95	0.01	−1.5 to +1.5
3	13.6	7.89	12.02	0.01	−1.5 to +1.5
4	15.7	10.05	17.34	0.01	−1.5 to +1.5
5	40.9	14.14	25.12	0.01	−1.5 to +1.5
6	58.6	14.76	25.98	0.01	−1.5 to +1.5
7	83.0	16.31	28.47	0.01	−1.5 to +1.5
8	109.8	18.47	32.09	0.01	−1.5 to +1.5
9	188.9	22.80	39.2	0.01	−1.5 to +1.5
10	367.3	27.97	48.0	0.01	−1.5 to +1.5
11	386	29.30	51.39	0.01	−1.5 to +1.5
12	461	31.46	55.65	0.01	−1.5 to +1.5
13	667.6	33.63	59.77	0.01	−1.5 to +1.5
14	1061	44.04	78.06	0.01	−1.5 to +1.5

different concentrations of standard hydrogen peroxide (Fig. S4). The detection results are listed in Table 1. Recoveries from different serum samples are in the range of 95% to 103.4%.

3.5. Quantitative determination of H_2O_2 from serum samples of ovarian cancer patients

Finally, Cat@AMQDs-GCE is used for the quantitative determination of hydrogen peroxide from serum samples of ovarian cancer patients. Before electrochemical analysis, fourteen samples are tested by Elecsys CA 125 II Assay to determine the level of CA125 in serum samples. All the samples have different levels of CA125 (Table 2). After assessing the CA125 levels in all serum samples, concentration of H_2O_2 is measured by cyclic voltammetry using Cat@AMQDs-GCE under optimized experimental conditions (potential range of −1.5 V to 1.5 V). It has been reported previously that concentration of hydrogen peroxide is directly related to CA125 levels and H_2O_2 concentration indifferent types of cancers is in micro or submicromolar levels [49,50]. From the obtained current values, concentration of hydrogen peroxide in each sample is calculated. With increasing level of CA125 in serum samples, concentration of H_2O_2 also increases (Table 2). Maximum hydrogen peroxide concentration is detected in the sample having CA125 level 1061 units.mL^{-1}. 46 units.mL^{-1} of CA 125 is considered normal concentration in serum sample, above that is the indication of benign cancer. The results indicate that cancer stage can be predicted by detecting hydrogen peroxide in serum samples through the developed biosensing method.

4. Conclusion

Hydrogen peroxide is a predictive biomarker of different types of cancers and also linked to CA125 levels. A novel biosensor is developed based on antimonene quantum dots (AMQDs) immobilized with catalase to monitor the hydrogen peroxide concentrations. Synthesis of AMQDs is simple and this material is used for the first time in electrochemical sensing applications. Catalase is specific to hydrogen peroxide. After characterization by TEM, AFM, SEM, EDS, XRD and FTIR, Cat@AMQDs-GCE is used for the electrochemical sensing of hydrogen peroxide. Material shows excellent redox behavior for H_2O_2 with LOD as 4.4 μM, linearity up to 0.989 and recovery of 95% to 103.4%. Cat@AMQDs-GCE works best in physiological pH of 7, ideal for biological analysis. Modified electrode is selective in the presence of interfering species such as dopamine, ascorbic acid, glucose and leucine. It is stable up to 30 cycles with no significant change in redox behavior, demonstrating the reproducibility and reusability. Material is applied for the quantitative determination of hydrogen peroxide from ovarian cancer serum samples in which CA125 levels are prediagnosed by Elecsys CA 125 II Assay. Determined H_2O_2 concentrations are comparable to the reported concentrations of H_2O_2 which translates its capability as biosensing material in clinical diagnosis.

CRediT author statement

Batool Fatima: Conceptualization, Methodology, Writing. **Dilshad Hussain**: Writing, Methodology, Conceptualization. **Shazia Bashir**: Investigation, Data Interpretation. **Hafiza Tanzilla Hussain**: Methodology, Characterization. **Rashida Aslam**: Execution, Data Recording. **Rahat Nawaz**: Methodology, Visualization. **Hafiza Nadia Rashid**: Writing, Data Compilation. **Nabila Bashir**: Investigation, Project Administration. **Saadat Majeed**: Software, Data Curation. **Muhammad Naeem Ashiq**: Conceptualization, Resource, Validation. **Muhammad Najam-ul-Haq**: Conceptualization, Writing- Reviewing and Editing, Supervision.

Declaration of competing interest

The authors declare that they have no known competing financial interests or personal relationships that could have appeared to influence the work reported in this paper.

Acknowledgements

Authors acknowledge Higher Education Commission (HEC), Pakistan for financial support and Nishtar Hospital Multan, Pakistan for providing serum samples of ovarian cancer patients. Furthermore, authors declare no conflict of interest.

Appendix A. Supplementary data

Supplementary data to this article can be found online at https://doi.org/10.1016/j.msec.2020.111296.

References

[1] J. Ferlay, I. Soerjomataram, R. Dikshit, S. Eser, C. Mathers, M. Rebelo, D.M. Parkin, D. Forman, F. Bray, Cancer incidence and mortality worldwide: sources, methods and major patterns in GLOBOCAN 2012, Int. J. Cancer 136 (5) (2015) E359–E386.
[2] G.M. Calaf, U. Urzua, L. Termini, F. Aguayo, Oxidative stress in female cancers, Oncotarget 9 (34) (2018) 23824.
[3] J. Kruk, H.Y. Aboul-Enein, Reactive oxygen and nitrogen species in carcinogenesis: implications of oxidative stress on the progression and development of several cancer types, Mini-Rev. Med. Chem. 17 (11) (2017) 904–919.
[4] P. Poprac, K. Jomova, M. Simunkova, V. Kollar, C.J. Rhodes, M. Valko, Targeting free radicals in oxidative stress-related human diseases, Trends Pharmacol. Sci. 38 (7) (2017) 592–607.
[5] S.B. Nimse, D. Pal, Free radicals, natural antioxidants, and their reaction mechanisms, RSC Adv. 5 (35) (2015) 27986–28006.
[6] M.-H. Pan, C.-T. Ho, Chemopreventive effects of natural dietary compounds on cancer development, Chem. Soc. Rev. 37 (11) (2008) 2558–2574.
[7] J.R. Stone, S. Yang, Hydrogen peroxide: a signaling messenger, Antioxid. Redox Signal. 8 (3–4) (2006) 243–270.
[8] K.P. Burton, Evidence of direct toxic effects of free radicals on the myocardium, Free Radic. Biol. Med. 4 (1) (1988) 15–24.
[9] D. Bandyopadhyay, A. Chattopadhyay, G. Ghosh, A.G. Datta, Oxidative stress-induced ischemic heart disease: protection by antioxidants, Curr. Med. Chem. 11 (3) (2004) 369–387.
[10] K. Cohen, A. Nyska, Oxidation of biological system: oxidative stress phenomena,

antioxidants, redox reactions and method for their quantification, Toxicol. Pathol. 30 (2002) 620–650.
[11] M. López-Lázaro, Dual role of hydrogen peroxide in cancer: possible relevance to cancer chemoprevention and therapy, Cancer Lett. 252 (1) (2007) 1–8.
[12] H. Sies, Hydrogen peroxide as a central redox signaling molecule in physiological oxidative stress: oxidative eustress, Redox Biol. 11 (2017) 613–619.
[13] Y. Wang, R. Branicky, A. Noë, S. Hekimi, Superoxide dismutases: dual roles in controlling ROS damage and regulating ROS signaling, J. Cell Biol. 217 (6) (2018) 1915–1928.
[14] B. Burek, S. Bormann, F. Hollmann, J. Bloh, D. Holtmann, Hydrogen peroxide driven biocatalysis, Green Chem. 21 (2019) 3232–3249.
[15] M.P. Lisanti, U.E. Martinez-Outschoorn, Z. Lin, S. Pavlides, D. Whitaker-Menezes, R.G. Pestell, A. Howell, F. Sotgia, Hydrogen peroxide fuels aging, inflammation, cancer metabolism and metastasis: the seed and soil also needs "fertilizer", Cell Cycle (Georgetown, Tex.) 10 (15) (2011) 2440–2449.
[16] F. Wen, Y. Dong, L. Feng, S. Wang, S. Zhang, X. Zhang, Horseradish peroxidase functionalized fluorescent gold nanoclusters for hydrogen peroxide sensing, Anal. Chem. 83 (4) (2011) 1193–1196.
[17] D. Jacewicz, K. Siedlecka-Kroplewska, J. Drzeżdżon, A. Piotrowska, D. Wyrzykowski, A. Tesmar, K. Żamojć, L. Chmurzyński, Method for detection of hydrogen peroxide in HT22 cells, Sci. Rep. 7 (1) (2017) 45673.
[18] S. He, W. Shi, X. Zhang, J. Li, Y. Huang, β−Cyclodextrins-based inclusion complexes of CoFe2O4 magnetic nanoparticles as catalyst for the luminol chemiluminescence system and their applications in hydrogen peroxide detection, Talanta 82 (1) (2010) 377–383.
[19] W. Chen, J. Chen, Y.-B. Feng, L. Hong, Q.-Y. Chen, L.-F. Wu, X.-H. Lin, X.-H. Xia, Peroxidase-like activity of water-soluble cupric oxide nanoparticles and its analytical application for detection of hydrogen peroxide and glucose, Analyst 137 (7) (2012) 1706–1712.
[20] A.A. Ensafi, F. Rezaloo, B. Rezaei, Electrochemical sensor based on porous silicon/silver nanocomposite for the determination of hydrogen peroxide, Sensors Actuators B Chem. 231 (2016) 239–244.
[21] C. Cheng, C. Zhang, X. Gao, Z. Zhuang, C. Du, W. Chen, 3D network and 2D paper of reduced graphene oxide/Cu2O composite for electrochemical sensing of hydrogen peroxide, Anal. Chem. 90 (3) (2017) 1983–1991.
[22] J. Yuan, S. Xu, H.-Y. Zeng, X. Cao, A.D. Pan, G.-F. Xiao, P.-X. Ding, Hydrogen peroxide biosensor based on chitosan/2D layered double hydroxide composite for the determination of H2O2, Bioelectrochemistry 123 (2018) 94–102.
[23] Y. Luo, H. Liu, Q. Rui, Y. Tian, Detection of extracellular H2O2 released from human liver cancer cells based on TiO2 nanoneedles with enhanced electron transfer of cytochrome c, Anal. Chem. 81 (8) (2009) 3035–3041.
[24] M. Jahanbakhshi, Myoglobin immobilized on mesoporous carbon foam in a hydrogel (selep) dispersant for voltammetric sensing of hydrogen peroxide, Microchim. Acta 185 (2) (2018) 121.
[25] Z. Deng, Y. Gong, Y. Luo, Y. Tian, WO3 nanostructures facilitate electron transfer of enzyme: application to detection of H2O2 with high selectivity, Biosens. Bioelectron. 24 (8) (2009) 2465–2469.
[26] P. Prabhu, R.S. Babu, S.S. Narayanan, Synergetic effect of Prussian blue film with gold nanoparticle graphite–wax composite electrode for the enzyme-free ultrasensitive hydrogen peroxide sensor, J. Solid State Electrochem. 18 (4) (2014) 883–891.
[27] B. Li, H.-Y. Song, Z.-P. Deng, L.-H. Huo, S. Gao, Novel sensitive amperometric hydrogen peroxide sensor using layered hierarchical porous α-MoO3 and GO modified glass carbon electrode, Sensors Actuators B Chem. 288 (2019) 641–648.
[28] K. Cui, Y. Song, Y. Yao, Z. Huang, L. Wang, A novel hydrogen peroxide sensor based on Ag nanoparticles electrodeposited on DNA-networks modified glassy carbon electrode, Electrochem. Commun. 10 (4) (2008) 663–667.
[29] S.T.R. Naqvi, B. Shirinfar, D. Hussain, S. Majeed, M.N. Ashiq, Y. Aslam, N. Ahmed, Electrochemical sensing of ascorbic acid, hydrogen peroxide and glucose by bimetallic (Fe, Ni)−CNTs composite modified electrode, Electroanalysis 31 (5) (2019) 851–857.
[30] X.-m. Chen, Z.-x. Cai, Z.-y. Huang, M. Oyama, Y.-q. Jiang, X. Chen, Ultrafine palladium nanoparticles grown on graphene nanosheets for enhanced electrochemical sensing of hydrogen peroxide, Electrochim. Acta 97 (2013) 398–403.
[31] M.-J. Song, S.W. Hwang, D. Whang, Non-enzymatic electrochemical CuO nanoflowers sensor for hydrogen peroxide detection, Talanta 80 (5) (2010) 1648–1652.
[32] L.C. Jiang, W.D. Zhang, Electrodeposition of TiO2 nanoparticles on multiwalled carbon nanotube arrays for hydrogen peroxide sensing, Electroanalysis 21 (8) (2009) 988–993.
[33] F. Jiang, R. Yue, Y. Du, J. Xu, P. Yang, A one-pot 'green' synthesis of Pd-decorated PEDOT nanospheres for nonenzymatic hydrogen peroxide sensing, Biosens. Bioelectron. 44 (2013) 127–131.
[34] D. Chirizzi, M.R. Guascito, E. Filippo, C. Malitesta, A. Tepore, A novel nonenzymatic amperometric hydrogen peroxide sensor based on CuO@ Cu2O nanowires embedded into poly (vinyl alcohol), Talanta 147 (2016) 124–131.
[35] S.T. Raza Naqvi, B. Shirinfar, S. Majeed, M. Najam-ul-Haq, D. Hussain, T. Iqbal, N. Ahmed, Synthesis, design and sensing applications of nanostructured ceria-based materials, Analyst 143 (23) (2018) 5610–5628.
[36] Y. Li, J.-J. Zhang, J. Xuan, L.-P. Jiang, J.-J. Zhu, Fabrication of a novel nonenzymatic hydrogen peroxide sensor based on Se/Pt nanocomposites, Electrochem. Commun. 12 (6) (2010) 777–780.
[37] T. Wen, F. Qu, N.B. Li, H.Q. Luo, Polyethyleneimine-capped silver nanoclusters as a fluorescence probe for sensitive detection of hydrogen peroxide and glucose, Anal. Chim. Acta 749 (2012) 56–62.
[38] X. Jiang, H. Jin, Y. Sun, Z. Sun, R. Gui, Assembly of black phosphorus quantum dots-doped MOF and silver nanoclusters as a versatile enzyme-catalyzed biosensor for solution, flexible substrate and latent fingerprint visual detection of baicalin, Biosens. Bioelectron. 112012 (2020).
[39] R. Gui, H. Jin, Y. Sun, X. Jiang, Z. Sun, Two-dimensional group-VA nanomaterials beyond black phosphorus: synthetic methods, properties, functional nanostructures and applications, J. Mater. Chem. A 7 (45) (2019) 25712–25771.
[40] H. Jin, R. Gui, J. Gong, W. Huang, Aptamer and 5-fluorouracil dual-loading Ag2S quantum dots used as a sensitive label-free probe for near-infrared photoluminescence turn-on detection of CA125 antigen, Biosens. Bioelectron. 92 (2017) 378–384.
[41] X. Bu, Y. Fu, H. Jin, R. Gui, Specific enzymatic synthesis of 2, 3-diaminophenazine and copper nanoclusters used for dual-emission ratiometric and naked-eye visual fluorescence sensing of choline, New J. Chem. 42 (21) (2018) 17323–17330.
[42] Y. Gao, W. Tian, C. Huo, K. Zhang, S. Guo, S. Zhang, X. Song, L. Jiang, K. Huo, H. Zeng, Tailoring natural layered β-phase antimony into few layer antimonene for Li storage with high rate capabilities, J. Mater. Chem. A 7 (7) (2019) 3238–3243.
[43] W. Tao, X. Ji, X. Xu, M.A. Islam, Z. Li, S. Chen, P.E. Saw, H. Zhang, Z. Bharwani, Z. Guo, J. Shi, O.C. Farokhzad, Antimonene quantum dots: synthesis and application as near-infrared photothermal agents for effective cancer therapy, Angew. Chem. Int. Ed. 56 (39) (2017) 11896–11900.
[44] T. Xue, W. Liang, Y. Li, Y. Sun, Y. Xiang, Y. Zhang, Z. Dai, Y. Duo, L. Wu, K. Qi, B.N. Shivananju, L. Zhang, X. Cui, H. Zhang, Q. Bao, Ultrasensitive detection of miRNA with an antimonene-based surface plasmon resonance sensor, Nat. Commun. 10 (1) (2019) 28.
[45] P. Ares, J.J. Palacios, G. Abellán, J. Gómez-Herrero, F. Zamora, Recent progress on antimonene: a new bidimensional material, Adv. Mater. 30 (2) (2018) 1703771.
[46] R. Aslam, B. Fatima, D. Hussain, R. Nawaz, S. Majeed, M.N. Ashiq, T.I. Qureshi, M. Najam-Ul-Haq, Sensitive and high recovery electrochemical sensing of resorcinol by Cd–glutathione complex-modified glassy carbon electrode, Int. J. Environ. Anal. Chem. (2020) 1–11.
[47] L.A. Torre, F. Islami, R.L. Siegel, E.M. Ward, A. Jemal, Global cancer in women: burden and trends, Cancer Epidemiol. Biomark. Prev. 26 (4) (2017) 444.
[48] S. Singh, M. Singh, K. Mitra, R. Singh, S.K. Sen Gupta, I. Tiwari, B. Ray, Electrochemical sensing of hydrogen peroxide using brominated graphene as mimetic catalase, Electrochim. Acta 258 (2017) 1435–1444.
[49] G. Vilema-Enriquez, A. Arroyo, M. Grijalva, R.I. Amador-Zafra, J. Camacho, Molecular and cellular effects of hydrogen peroxide on human lung cancer cells: potential therapeutic implications, Oxidative Med. Cell. Longev. 2016 (2016) 1908164.
[50] C. Zong, M. Wang, B. Li, X. Liu, W. Zhao, Q. Zhang, A. Liang, Y. Yu, Sensing of hydrogen peroxide and glucose in human serum via quenching fluorescence of biomolecule-stabilized Au nanoclusters assisted by the Fenton reaction, RSC Adv. 7 (43) (2017) 26559–26565.